Adaptive Threshold and Piecewise Fitting for Iris Localisation

Zuraini Othman[1] and Azizi Abdullah[2]

[1]Department of Intelligent Computing and Analytics, Faculty of Information & Communication Technology, Universiti Teknikal Malaysia Melaka, Hang Tuah Jaya, 76100 Durian Tunggal,Melaka, Malaysia.
[2]Center for Artificial Intelligence Technology, Faculty of Information Science and Technology, Universiti Kebangsaan Malaysia 43600 Bangi, Selangor Darul Ehsan, Malaysia.
zuraini@utem.edu.my

Abstract— **Machine vision needs detectors to get features and properties of objects in each image to be used for ensuring the effectiveness of each study conducted. The most recognisable Canny edge detection method aims to lessen noise and eliminate unwanted edge by employing threshold values and hysteresis for localisation advantages. Canny method uses a high threshold and a low threshold to decrease of false positive pixel edges and to describe the contours in the image crucially as compared to use one fixed threshold value for the maximum gradient is not the best option. Nevertheless, using two unchanged threshold values still do not guarantee to provide the best results because the image contains huge variations. Previously, adaptive thresholds have been introduced for specific domain only. Here, a technique to determine the threshold values from the foreground and background image pixels in the global and local image will be used for further analysis. This approach involves partitioning an image into several similar size blocks at multiple resolution levels. Then, a sampling procedure uses on global and local images to acquire the best threshold value by selecting the highest between the class variance values. Finally, piecewise cubic spline will completely segment the boundary for iris and pupil region. Experiments have been done on CASIA V2 datasets. The results show that edge image obtained outperform the Canny method and previous work. Iris localization image obtained also more accurate compared to Hough method.**

Index Terms— **Edge Detection; Global and Local Approaches; Multiple Resolutions; Piecewise Cubic Spline; Threshold Value.**

I. INTRODUCTION

In iris recognition system, the most important step is to obtain accurate iris localisation from eye image. Hence, the information of edges obtained from each image plays an essential part in the analysis of image properties. Thus, the study of effective image information has become one of the major areas of research among researchers.

Edge detection reduces the amount of data and filters noise in the image and the important features of the image will be considered. The most commonly used methods in this area are Canny, Sobel, Prewitt, Log and Laplace methods. Each of these methods has their ability in controlling a simpler and less computational algorithm. However, there are certain drawbacks to those methods[1].

Canny method introduced by [2] has excellent performance and mostly used in practice. This approach smoothed the image by using Gaussian filter by smoothing the high frequent signals that may the edge pixels exist and made the loss of edge details while suppressing the noise. Furthermore, in this approach the high and low thresholds have to be set manually and requiring earlier empirical research, and many experiments need in order to get possible proper threshold. However, in the real application the low and high thresholds are frequently changed due to the different illumination and scenes in nature of each image. In many cases the conventional canny operator lack of the self-adaptation capability to obtain satisfying detection results [3].

There are studies on edge based and threshold based segmentation, a Canny edge detector is considered to be an example of the first method and Otsu [4] thresholding represent the other method done by [5], [6]. Otsu method based on a gray level histogram which is deduced by the least square method. It is the most stable method in the image threshold segmentation at present and in the statistical sense, this method also has the best threshold value [7]. In order to make Canny adaptively select the high threshold (H_t) and low threshold (L_t) value, Otsu method will be used such as research done by[3], [7]–[11].

Fixed partitioning approach is thoroughly used to analyse the image globally and locally in order to obtain the local spatial value of an image. By using this approach, the image is partitioned into the same size blocks and for each block the local histogram will be computed. The main advantage of this method is to obtain the spatial distribution of image content so that an extra input to the histogram will be provided [12]. In this proposed method, a comprehensive technique has been used in order to produce edges for data of iris images. The iris localisation is frequently used to determine the boundaries of iris and pupil. These boundaries have been modelled with circles, ellipses, and splines. Intuitively, the more accurate model could produce better recognition performance and this becomes the basis in the selection of widely used spline methods in the area of iris recognition to estimate iris and pupil boundaries [13].

In this paper, we propose an algorithm for finding edge images from iris image dataset in five different fixed partitioning image levels by using an adaptive threshold approach based on local spatial value. Otsu method will be used to determine the high and the low threshold values. Different from [9], here the maximum value from all H_t and L_t generated will be selected. The best edge images obtained are measured by comparing with the ground truth images which have been validated by experts. The unconnected boundaries will be completely segmented by the piecewise cubic spline interpolation. The result of the experiment will

be compared with the Canny method and previous work[9]. It shows that the proposed method gives the most accurate edge images. Datasets from CASIA V2[14] will be used in this experiment.

II. MATERIALS AND METHODS

Canny edge detection will be used on selecting the edge by getting assistance from Otsu method on selecting threshold values. Furthermore, sampling approach on selecting the variance values will be used to analyses the image globally and locally use multiple resolution techniques in order to get more self-adaptive threshold values. Furthermore, a smoothing spline based edge fitting scheme is presented to deal with non-circular iris boundaries. Methods used in this study are as follows:

A. Canny edge detection

Currently, the canny edge detector is known as one of the best edge detectors[5]. In summary, good detection, good localisation and only one response to a single edge are the criteria's in canny edge detection[2]:

Tradition Canny algorithm consists of the following steps[3], [15].

The gaussian filter will be used for smoothing image for restraining noise.

The finite difference on the first order partial derivative for calculating the gradient magnitude $M(x, y)$ and the gradient direction $H(x, y)$ of the image. $M(x, y)$ is defined as follow:

$$M(x, y) = \sqrt{E_x(x, y)^2 + E_y(x, y)^2} \tag{1}$$

The H(x, y) is defined as follow:

$$H(x, y) = \arctan(E_x(x, y) / E_y(x, y)) \tag{2}$$

where, E_x and E_y is the result of the image being affected by the filter along the row-column direction.

Non-maximum suppression is done for the gradient magnitude while the dual-threshold algorithm is adopted to detect and connect edges. Next, hysteresis is done in order to determine final edges by supressing all edges that are not connected to a very strong edge.

The drawback of traditional canny edge detection is the H_t and L_t are set manually requiring prior empirical knowledge, and it is possible to get a proper threshold after many experiments. However, in practice, the H_t and L_t often change because of the scenes and illumination change frequently[3].

Here, modified Canny edge detection will be used to make self-adaptive on choosing H_t and L_t values rather than traditional canny edge detection which manually selects the value of H_t and L_t. Therefore, Otsu method will be applied to get the value of H_t and L_t.

B. Otsu method

Otsu threshold is used in many applications from medical imaging to a low level in computer vision. It is because of the ease of implementation and the relative complexity[5].

From [4], let the pixel of given picture in L gray levels $[1,2,...,L]$. The number of pixels at level i is denoted as n_i and a total number of pixels as $N = n_1 + n_2 + ... + n_L$. Then normalized the gray level histogram and considered as a probability distribution:

$$p_i = \frac{n_i}{N}, p_i \geq 0, \sum_{i=1}^{L} p_i = 1 \tag{3}$$

Otsu is based on the threshold for partitioning the image pixels into two classes C_0 and C_1 (background and object or vice versa) at level t, where: $C_0 = \{1,2,...,t\}$ and $C_1 = \{t+1, t+2, ..., L\}$. Then the probabilities (Pr) of class occurrence are

$$C_0 = \Pr(C_0) = \sum_{i=1}^{t} p_i = \omega(t) \tag{4}$$

$$\omega_1 = \Pr(C_1) = \sum_{i=t+1}^{L} p_i = 1 - \omega(t) \tag{5}$$

and the Pr of class mean levels are

$$\mu_0 = \sum_{i=1}^{t} i \Pr(i|C_0) = \sum_{i=1}^{t} \frac{ip_i}{\omega_0} = \frac{\mu(t)}{\omega(t)} \tag{6}$$

$$\mu_1 = \sum_{i=t+1}^{L} i \Pr(i|C_1) = \sum_{i=t+1}^{L} \frac{ip_i}{\omega_1} = \frac{\mu_T - \mu(t)}{1 - \omega(t)} \tag{7}$$

where

$$\omega(t) = \sum_{i=1}^{t} P_i, \mu(t) = \sum_{i=1}^{t} ip_i \text{ and } \mu_T = \mu(L) = \sum_{i=1}^{L} ip_i \tag{8}$$

The class variances are

$$\sigma_0^2 = \sum_{i=1}^{t}(i - \mu_0)^2 \Pr(i|C_0) = \sum_{i=1}^{t} \frac{(i-\mu_0)^2 p_i}{\omega_0} \tag{9}$$

$$\sigma_1^2 = \sum_{i=t+1}^{L}(i - \mu_1)^2 \Pr(i|C_1) = \sum_{i=t+1}^{L} \frac{(i-\mu_1)^2 p_i}{\omega_1} \tag{10}$$

The between class variance is

$$\sigma_b^2 = \omega_0(\mu_0 - \mu_T)^2 + \omega_1(\mu_1 - \mu_T)^2 = \omega_0\omega_1(\mu_1 - \mu_0)^2 \tag{11}$$

and from (11) the optimal threshold t^* can be obtained by

$$\sigma_b^2(t^*) = \max_{1 \leq t < L} \sigma_b^2(t) \tag{12}$$

In the adaptive method by [7], [10] the value of t^* obtained will be used as Ht value in Canny edge detection, given as

$$H_t = t^* \tag{13}$$

In order to auto calculate the value of L_t, the value is given by [7]

$$L_t = \frac{1}{2} H_t \tag{14}$$

In this proposed method, there was weight (n) within some range introduced on every selection of H_t and L_t values. It will be given more choices of values so that more accurate edge detection image will be obtained.

a) Curve Fitting Method

Here, smoothing spline will be used to fit the uncomplete

boundaries. Let N be detected edge boundaries and $\{x_i\}_{i=0}^{N-1}$ are generally imperfectly detected with a confidence interval $[x_i - \sigma, x_i + \sigma]$. Cubic smoothing spline is an excellent way to achieve this goal. A cubic spline is a piecewise continuous curve. There is a separate cubic polynomial for each interval $[x_i, x_{i+1}]$:

$$S_i(x) = a_i(x - x_i)^3 + b_i(x - x_i)^2 + c_i(x - x_i) + d_i \quad (15)$$

for $x \in [x_i, x_{i+1}]$, these polynomial segments are denoted as $S(x)$ [16].

A cubic smoothing spline is formed for the minimum of the function:

$$\alpha \sum_{i=0}^{N-1} \frac{[rx_i - S(x_i)]^2}{\sigma^2} + \beta \int |S''(x)|^2 \, dx \quad (16)$$

Equation (16) can be rewritten after simplification as

$$\rho \sum_{i=0}^{N-1} w_i [x_i - S(x_i)]^2 + (1-\rho) \int |S''(x)|^2 \, dx \quad (17)$$

where weight w default value as 1 for all data points. The first part in equation (17) computes the closeness spline with the edge data, and the second part computes the roughness of the spline fitting. The smoothing parameter ρ controls the relative weight on $S(x)$ close to the data by having $S(x)$ smooth accordingly. By putting $\rho = 0$ allows $S(x)$ becomes a least-squares straight line, whereas putting $\rho = 1$ allows $S(x)$ becomes cubic spline interpolant [17].

III. ADAPTIVE THRESHOLD AND PIECEWISE FITTING FOR IRIS LOCALISATION

After retrieved original images, these images will be transformed to gray level images. The image is then fix partitioned into five different levels. Otsu method will be adopted in Canny edge detection in order to select threshold value but some changes have been done in order to obtain the best H_t value and low L_t value. By using various resolutions of images, selection on variance values for global spatial value L_1 and local spatial value in L_2, L_3, L_4 and L_5 are carried out.
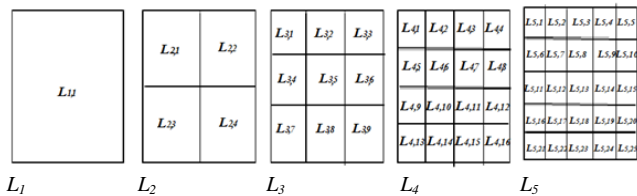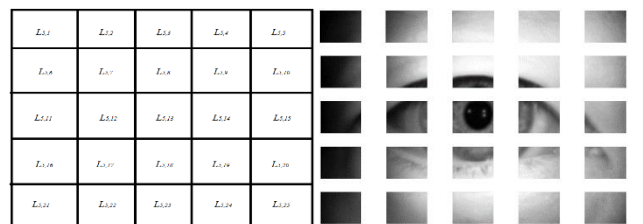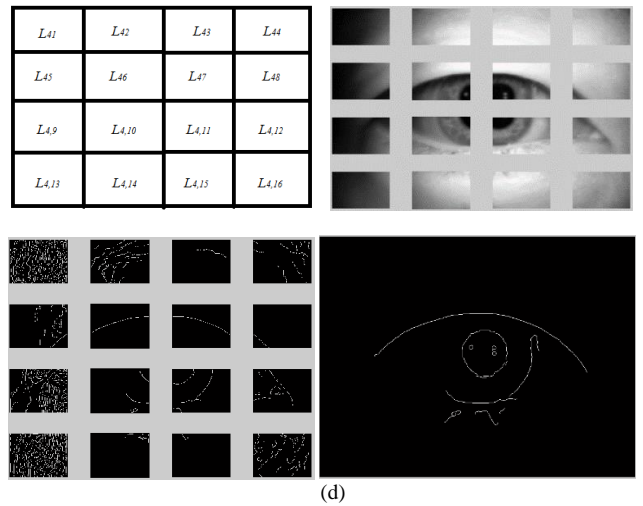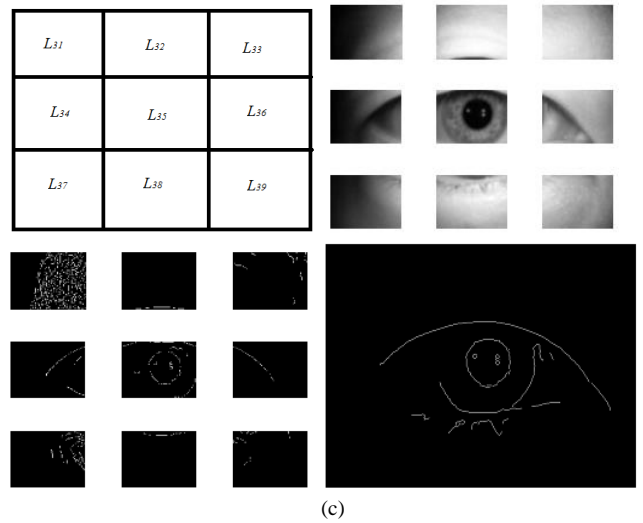

Figure 1: Fixed partitioning on images
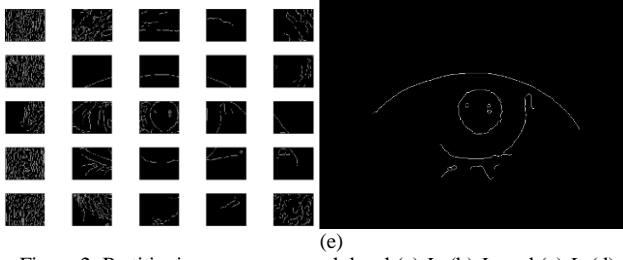

(a)

(b)

(c)

(d)

(e)
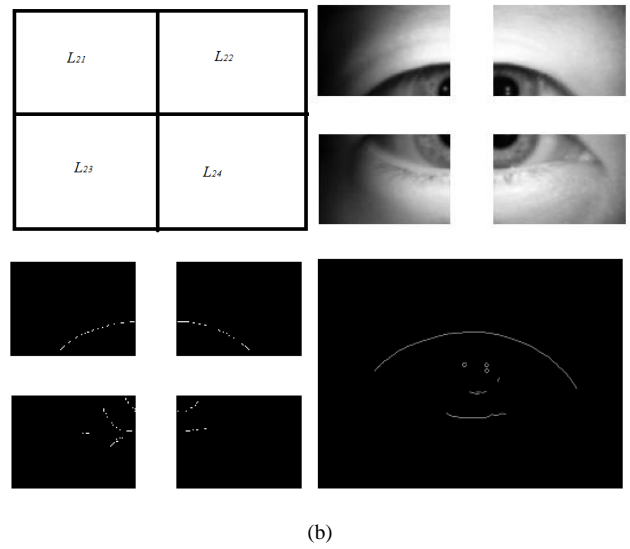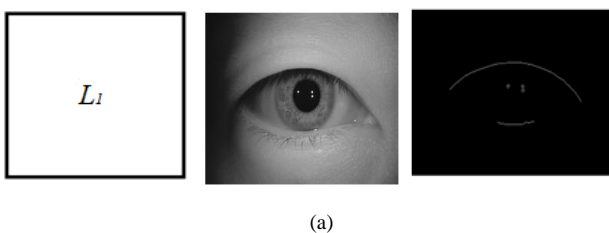
Figure 2: Partitioning process on each level (a) L_1,(b) L_2 and (c) L_3 (d) L_4 and (e) L_5

Let L be a partition $m \times m$ image and it is depicted as image partition in each level L_m where $m = 1,2,...,5$. For each level, partition L_{mj} will provide spatial local H_t and L_t values where $j = 1,2,...,m^2$ (see Figure 1 and Figure 2). Different from work done by [9] even though global analysed images L_1, H_t and L_t will be obtained directly same as work done by [3] from equation (13) and equation (14) above. Here, all level will go through the same processes. The proposed approach uses this concept to fix the partitioning in each L_m image as carried out in [10]. Here, weight is introduced (where $n = 1,2,3,...,10.$) in determining the spatial H_t and L_t values in every global (L_1) and local (L_2, L_3, L_4 and L_5) partition. In each L_{mj} the maximum value of H_t (HS_t) and the maximum value of L_t (LS_t) will be selected except (for L_1 because there is only 1 partition involved). For global image L_1 (see Figure 2 (a)):

$$HS_t = \frac{1}{n} \times H_t \quad (18)$$

and from equation (13)

$$LS_t = \frac{1}{n}\left(\frac{1}{2} H_t\right) \quad (19)$$

For L_2, L_3, L_4 and L_5

$$HS_t = \frac{1}{n} \times \arg\max(H_t \in L_{mj}) \quad (20)$$

Then, the corresponding L_t for each L_{mj} is

$$L_t = \frac{1}{2} H_t \text{ for each } H_t \in L_{mj} \quad (21)$$

Next, the minimum value of L_t

$$LS_t = \frac{1}{n} \times \arg\max(L_t \in L_{mj}) \quad (22)$$

Hence after HS_t and LS_t generated, the process will continue with hysteresis phase to obtain the complete edge image (I). Furthermore, the most accurate edge image (I_t) is selected after comparing with the ground truth image provided.

$$I_t = \text{accurate}(I \in L_m) \quad (23)$$

Furthermore to complete the segmentation process, I_t will undergo the morphology process then the curve fitting process will be executed (see Figure 3).

(a) (b)
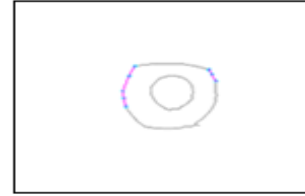
(c)

Figure 3: Segmentation process (a) I_t edge image (b) edge obtain after morphology process and (c) Segmented image

IV. EXPERIMENTS AND RESULTS

In this study the iris datasets from CASIA V2 has been used. The ground truth edge images are manually drawn and have been verified by optometrists from Hospital Melaka. So, in order to compare with the result from this experiment, edge images from the binary image provided have been produced. Here, the measurement is Figure of Merit (FOM) provided by Pratt [18], which is:

$$\text{FOM} = \frac{1}{\max(N_1, N_T)} \sum_{i=1}^{N_T} \frac{1}{1 + \alpha d_i^2} \quad (24)$$

where N_1 and N_T refer to the number of ideal and the actual edge points, while, d_i is the pixel Euclidean distance of the ith edge detected, and α is a scaling constant selected to be $\alpha = \frac{1}{9}$ and is used for penalising the displaced edges. Larger FOM values (values are between 0 and 1) indicate better performance in the resultant images.
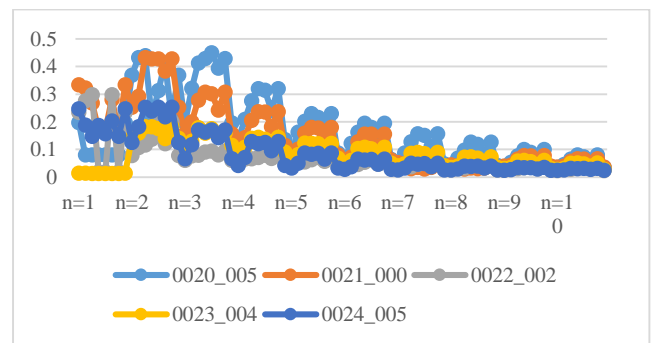

Figure 4. FOM graph on CASIA image 0020_005

Table 1
FOM values on CASIA image 0020_005

n	L_1	L_2	L_3	L_4	L_5
1	0.1979	0.0806	0.0805	0.0804	0.0804
2	0.3687	0.4331	0.4396	0.2166	0.3136
3	0.1971	0.3212	0.4136	0.4299	0.4502

4	0.1369	0.2092	0.2761	0.3207	0.3148
5	0.0874	0.1628	0.2029	0.2308	0.2164
6	0.0648	0.1226	0.1631	0.1952	0.1809
7	0.0489	0.0875	0.1283	0.1567	0.1512
8	0.0428	0.0688	0.0981	0.1268	0.1186
9	0.0389	0.0540	0.0775	0.1005	0.0898
10	0.0362	0.0463	0.0653	0.0811	0.0742

Here only $n = 1,2,3,...,10$ are considered because from the result of FOM in each dataset used shown in Figure 4 that the most accurate edge image (the highest FOM value) is contained in between that range. From equation (18)

$$I_t = \arg\max \left(\text{FOM}\left(I \in L_m\right)\right) \tag{25}$$

By using this method 50 I images produced which is more than the other adaptive method by [9], [10]. Table 1 shows the example of 50 FOM values generated for image 0020_005. The highest FOM value is in L_5 with $n = 3$ (highlighted).

Table 2
FOM values obtained from Canny, Sobel, Prewitt, Log and Robert method.

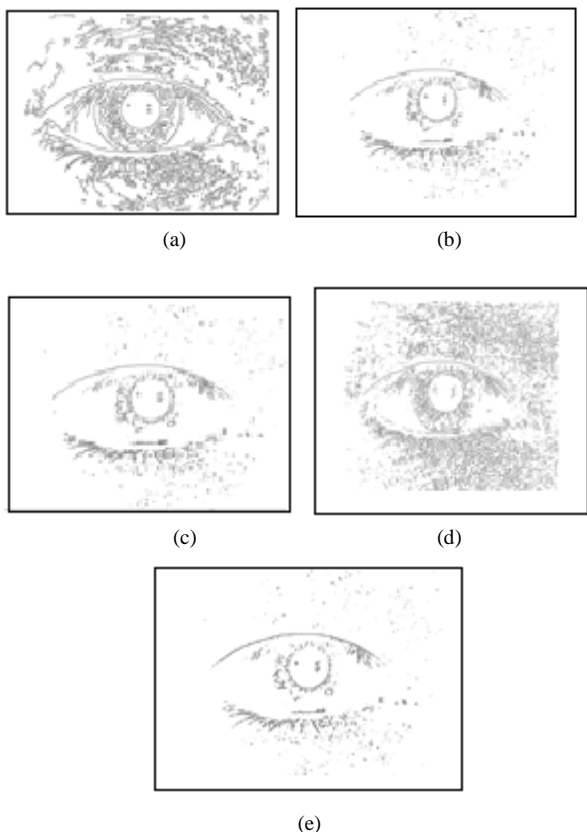| Image	Canny	Sobel	Prewitt	Log	Robert
0020_005	0.0445	0.1294	0.1308	0.0321	0.1477
0021_000	0.0323	0.1136	0.1160	0.0317	0.1564
0022_002	0.0304	0.0598	0.0596	0.0329	0.0669
0023_004	0.0377	0.0617	0.0626	0.0382	0.0624
0024_005	0.0471	0.1088	0.1100	0.0387	0.1127

(a)   (b)

(c)   (d)

(e)

Figure 4. Edge images obtained from image 002_005 (a) Canny method, (b) Sobel method, (c) Prewitt method, (d) Log method and (e) Robert method.

Table 2 shows the comparison on FOM values obtained from Canny, Sobel, Prewitt, Log and Robert method. From the result obtained, Robert method almost outperforms other methods except for image 0023_004 which is Prewitt method outperform other methods.. By referring to edge image obtained in Figure 4, the highest FOM produced less edges detected which is Robert method compared to the lowest FOM values produced a lot of edges detected which is from the Canny method. Even though, FOM values obtained from the Canny method are among the lowest values but the edge image obtained successfully detect almost all the iris and pupil boundaries.

Table 3
FOM values from Canny, previous work and the proposed method

Image	Canny	Previous work[9]	Proposed
0020_005	0.0445	0.4148	0.4502
0021_000	0.0323	0.4251	0.4333
0022_002	0.0304	0.2357	0.2986
0023_004	0.0377	0.1673	0.1833
0024_005	0.0471	0.2368	0.2532

Table 3 shows that the proposed method outperform the FOM values from previous work [9] and Canny method. The proposed method also outperforms the FOM values in Sobel, Prewitt, Log and Robert method in Table 2. Furthermore, as in Figure 5 image result obtained from image 002_005 shows that proposed method gave less noise image and iris boundaries are clearly detected compared to previous work [9] and other methods in Figure 4. Finally, the segmentation process by using piecewise cubic spline will be generated (as in Figure 6). Here, the comparison between proposed work and Hough method show that this two method localise iris and pupil boundaries well. However, in localised iris image obtained from proposed method produce iris boundaries without eyelid which near to the ground truth image.
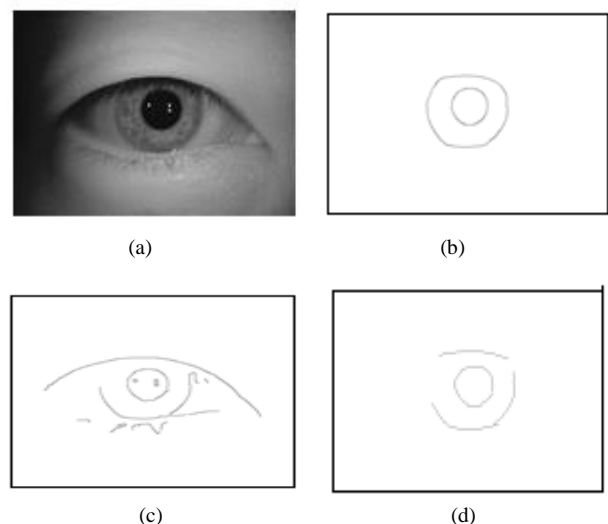

(a)   (b)

(c)   (d)

Figure 5. Image 002_005 (a) Original image (b) Ground truth image (c) Previous work[9] (d) Proposed method.
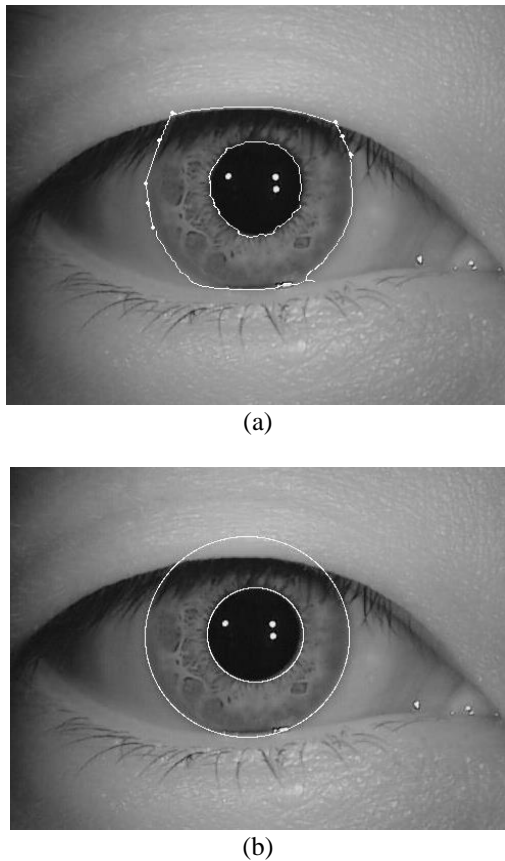
(a)

(b)

Figure 6. Segmented image obtained from image 002_005. (a) Proposed method and (b) Hough Method

V.   CONCLUSION

This paper proposes to localise iris method by applying self-adaptive threshold values selected with the aid of the Otsu method. Furthermore, the calculations have been carried out on images globally and locally using fixed partitioning and at multiple resolution levels. In order to get the optimal threshold value, a sampling approach has been used by calculating the maximum between class variance values from each partition block. Then, piecewise cubic spline fitting will be used to completely localise iris image.

The results show that from image datasets used, the proposed method outperforms the Canny, Sobel, Prewitt, Log, Robert and previous work in terms of FOM values and the edge image results obtained. Modification on Canny method has been chosen because edge image obtained gives the complete edge boundaries even though more unwanted edge detected. Here, proved that local spatial adaptive approach by using Otsu Method enhance the edge obtained by eliminating the noises required from the conventional Canny method. From the result of the image shows the

accurate edge image because it contains the edge image from the foreground and has ignored the edge image from the background. Finally the cubic spline interpolation completely localises the boundaries of pupil and iris in the image and eliminate the eyelid area wisely.

REFERENCES

[1]   M. Wang, J. S. Jin, Y. Jing, X. Han, L. Gao, and L. Xiao, "The Improved Canny Edge Detection Algorithm Based on an Anisotropic and Genetic Algorithm Mingjie," vol. 634, pp. 115–124, 2016.

[2]   J. Canny, "A computational approach to edge detection.," *IEEE Trans. Pattern Anal. Mach. Intell.*, vol. 8, no. 6, pp. 679–98, Jun. 1986.

[3]   G. Jie and L. Ning, "An Improved Adaptive Threshold Canny Edge Detection Algorithm," *2012 Int. Conf. Comput. Sci. Electron. Eng.*, pp. 164–168, Mar. 2012.

[4]   P. Smith, D. B. Reid, C. Environment, L. Palo, P. Alto, and P. L. Smith, "A Threshold Selection Method from Gray-Level Histograms," *IEEE Trans. Syst. Man. Cybern.*, vol. 9, no. 1, pp. 62–66, 1979.

[5]   Ali Abdo Mohammed Al-Kubati, J. A. M. Saif, and Murad A. A. Taher, "Evaluation of Canny and Otsu ImageSegmentation," *Int. Conf. Emerg. Trends Comput. Electron. Eng.*, pp. 23–25, 2012.

[6]   R. Anitha and S. Jyothi, "Classifying Penaeid Prawns Species using Canny and Otsu," *Int. J. Adv. Res. Comput. Sci. Manag. Stud.*, vol. 2, no. 11, pp. 35–42, 2014.

[7]   M. Fang, G. Yue, and Q. Yu, "The study on an application of otsu method in canny operator," *Int. Symp. Inf. …*, vol. 2, no. 4, pp. 109–112, 2009.

[8]   J. Zhao, H. Yu, X. Gu, and S. Wang, "The edge detection of river model based on self-adaptive Canny Algorithm and connected domain segmentation," *2010 8th World Congr. Intell. Control Autom.*, vol. 2, no. 1, pp. 1333–1336, Jul. 2010.

[9]   Z. Othman and A. Abdullah, "An Adaptive Threshold Based On Multiple Resolution Levels for Canny Edge Detection," in *IRICT 2017: Recent Trends in Information and Communication Technology*, 2017, pp. 316–323.

[10]   Z. Othman, A. Abdullah, and A. S. Prabuwono, "A statistical Approach of Multiple Resolution Levels for Canny Edge Detection," in *Intelligent Systems Design and Applications (ISDA), 2012*, 2012, pp. 837–841.

[11]   P. Hui, Z. Ruifang, L. Shanmei, W. Youxian, and W. Lanlan, "Edge Detection of Growing Citrus Based on Self-Adaptive Canny Operator," *2011 Int. Conf. Comput. Distrib. Control Intell. Environ. Monit.*, no. c, pp. 342–345, Feb. 2011.

[12]   A. Abdullah, R. C. Veltkamp, and M. a. Wiering, "Spatial pyramids and two-layer stacking SVM classifiers for image categorization: A comparative study," *Proc. Int. Jt. Conf. Neural Networks*, pp. 5–12, 2009.

[13]   Y. Zhao, C. Ti, X. Huang, A. Tokuta, and R. Yang, "A performance comparison between circular and spline-based methods for iris segmentation," *Proc. - Int. Conf. Pattern Recognit.*, pp. 351–356, 2014.

[14]   "CASIA-IrisV2." [Online]. Available: http://biometrics.idealtest.org/.

[15]   B. Wang and S. Fan, "An improved CANNY edge detection algorithm Bing," *2009 Second Int. Work. Comput. Sci. Eng.*, 2009.

[16]   C. H. Reinsch, "Smoothing by spline functions, II," *Numer. Math.*, vol. 16, no. 3, pp. 451–454, 1971.

[17]   Z. He, T. Tan, Z. Sun, and X. Qiu, "Towards Accurate and Fast Iris Segmentation for Iris Biometrics," *IEEE Trans. Pattern Anal. Mach. Intell.*, 2008.

[18]   I. E. Abdou and W. K. Pratt, "Quantitative Design and Evaluation of Enhancement/Thresholding Edge Detectors.," *Proc IEEE*, vol. 67, no. 5, pp. 753–763, 1979.